Bull. Mater. Sci., Vol. 38, No. 5, September 2015, pp. 1429–1433. © Indian Academy of Sciences.

Evaluation on electrical resistivity of silicon materials after electron beam melting

HAFIZ MUHAMMAD NOOR UL HUDA KHAN ASGHAR[1,2,3], SHUANG SHI[1,2], DACHUAN JIANG[1,2] and YI TAN[1,2,*]

[1]School of Materials Science and Engineering, Dalian University of Technology, Dalian 116023, PR China
[2]Key Laboratory for Solar Energy Photovoltaic System of Liaoning Province, Dalian 116023, PR China
[3]Department of Physics, Balochistan University of Information Technology, Engineering and Management Sciences, Quetta 87300, Pakistan

MS received 26 November 2014; accepted 12 May 2015

Abstract. This research deals with the study of electron beam melting (EBM) methodology utilized in melting silicon material and subsequently discusses on the effect of oxygen level on electrical resistivity change after EBM process. The oxygen content was reduced from 6.177 to less than 0.0517 ppmw when refining time exceeded 10 min with removal efficiency of more than 99.08%. The average value of electrical resistivity of silicon before EBM processing was recorded to be 2.25 Ω cm but with the increase in melting time that was applied through EBM, the electrical resistivity was recorded to go high in the range of 4–13 Ω cm for different regions. The electrical resistivity values were greater in the top and the bottom regions, whereas lowest in the central region at all conditions of melting time. It is the result of the evaporation of oxygen during melting process and the segregation of metal impurities during solidification.

Keywords. Electron beam melting; silicon; oxygen; removal; electrical resistivity.

1. Introduction

Multicrystalline silicon has now turned into the key material in the photovoltaic market because of its low production cost and high conversion efficiency of solar cells made from this material. The casting process is a cost-effective technique for large-scale production of multicrystalline silicon material.

Oxygen impurity is one of the main impurities in the crystal, which can be incorporated into silicon ingot during the casting process due to the reaction between silicon melt and quartz crucible at high temperature. The oxygen impurity can cause SiO_2 precipitation,[1] dislocation[2] and stacking faults[3,4] and can cause significant deterioration of the performance of solar cells.[5–8] Oxygen precipitation is known to act as intrinsic gettering sites for impurities and to affect mechanical strength of the wafer.[9,10] Oxygen can form a variety of inhomogeneous defects, such as thermal donors[11,12] due to the clusters of oxygen atoms[13,14] and some other donors due to the SiO_2 precipitates.[5,6] Except for those inhomogeneous defects, there is another kind of uniformly distributed defect: boron–oxygen complexes, which is responsible for an asymptotic, up to 10% degradation of solar cell performance by relative when the timescale of illumination is close to hours.[15,16] Effective control of oxygen concentrations in a crystal is required for the production of a high-quality crystal.

In recent times, a lot of research has been carried out on the purification of silicon using the electron beam melting (EBM) technique. Most of the impurities having evaporation coefficient greater than 1 can be removed most efficiently using EBM, such as aluminium, phosphorus and calcium.[17–21] It has been proved by the authors' previous research that by the increase in melting time, the amount of oxygen removal from silicon is increased.[22] However, till now, very few research works have enhanced the interesting relationship between electrical resistivity and the oxygen removal. In this paper, the distribution of electrical resistivity in silicon ingot with different melting times was measured. Based on the oxygen content results, the formation mechanism of the distribution behaviour was also discussed.

2. Experimental

The experiment was conducted in the EBM furnace. The furnace mainly consists of a chamber with a volume of 1 m^3, an electron beam gun with an accelerating voltage of 30 kV and maximum power of 30 kW, a water-cooled copper crucible with a diameter of 190 mm and depth of 50 mm, a circulating water-cooling system and a vacuum

*Author for correspondence (tanyi@dlut.edu.cn)

pump system. Two independent vacuum systems are employed in this furnace: one consists of mechanical pump, roots pump and diffusion pump for the chamber and the other consists of mechanical pump and diffusion pump for the electron gun.

The silicon samples were extracted from the bottom of a casted ingot, where it was characterized with the oxygen content of 6.177 ppmw and electrical resistivity was 2.25 Ω cm. Before melting electron beam, the sample was properly washed in alcohol by a supersonic wave cleaner in order to remove possible solid residues. For each experiment, 300 g of silicon was placed in a water-cooled copper crucible. After the pressure of the chamber and the electron beam gun was evacuated to less than 5.0×10^{-2} and 5.0×10^{-3} Pa, respectively. Later, the melting process was performed. The electron beam with a power of 15 kW was irradiated on the surface of the silicon until it was melted. Once silicon was melted completely, the electron beam was stopped instantaneously after the molten pool was held for a certain time. The melting time of zero was defined as the state in which the silicon was melted completely in the crucible. The silicon solidified in short time and was removed from the crucible after cooling for 30 min. The melting parameters are shown in table 1.

The silicon ingots were cut along the centre line and morphologies of the cross-sections were observed. The oxygen content levels were determined by secondary ion mass spectroscopy (SIMS) before and after EBM and the values of electrical resistivity was also measured by the four-probe method on four-point probe resistivity tester.

3. Results and discussion

3.1 *Oxygen content after EBM process*

The morphologies of the silicon ingot and oxygen content during different melting times are shown in figure 1. The raw material was extracted from the bottom of casted ingot; the values of oxygen concentration for different melting times have been measured by secondary ion mass spectrometry (SIMS) analysis. In SIMS we take a big sample for which the average value is used. Oxygen distribution was observed to be uniform throughout the samples for each melting time, in which the oxygen content was 6.177 ppmw. It was reduced to 1.629 ppmw (removal efficiency up to 73.6%) when silicon was melted completely at 15 kW, it decreased continually to less than 0.0517 ppmw (removal efficiency of more than 99.08%) when refining time exceeded 10 min, it must be less than 0.0517 ppmw. Whereas, after 20 and 30 min the amount of oxygen was detected to be the same as that of the 10 min. Although these numerical values owe to the limitation of SIMS, yet the EBM method is an effective and efficient process for oxygen removal from silicon, and the oxygen removal is enhanced with increased melting time.

Table 1. Melting parameters during EBM experiment.

Melting parameters	Value
Refining time (s)	0, 600, 1200 and 1800
Melting power (kW)	15
Chamber pressure (Pa)	5.0×10^{-2}
Irradiation pattern	Circular
Scanning frequency (Hz)	10

During solidification in the EBM process, the top and the bottom regions of the ingot solidify prior to the central region, which is due to the EBM principle. Solidification starts as the power is shut off. It is very quickly heading towards centre from the top and the bottom. It is very natural to solidify from the top because of vacuum space, but this process is quicker from the bottom, which is due to the circulation of cold water at the bottom (water-cooled copper crucible). Therefore, solidification from bottom to centre is more rapid as compared to the one from top to centre. This can also be seen from the interface formed in figure 1b–e, which is not exactly at the centre, but little bit more towards the top and a little bit more away from the bottom. The grain size is measured by image pro plus and it is similar in the same area for each ingot. That is to say, the effect of structure on the electrical resistivity is same, so the change of electrical resistivity can reflect the change of oxygen level.

3.2 *Electrical resistivity analysis*

The average values of electrical resistivity at different regions of each ingot are shown in figure 2. The cross-section of the quarter sample was divided into five equal

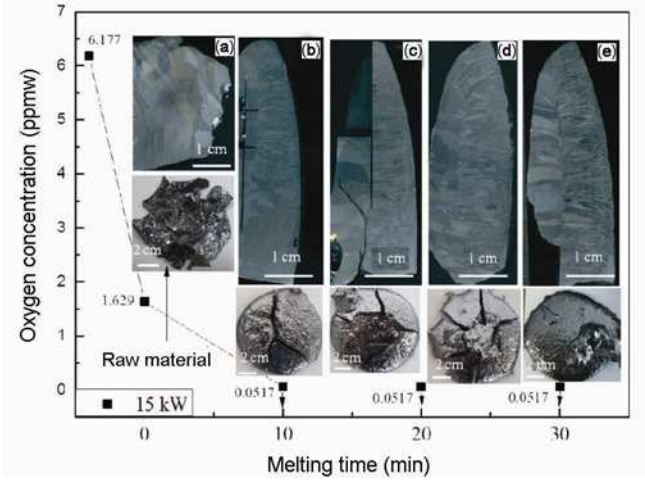

Figure 1. Oxygen content as a function of time and morphologies of the silicon ingot: (**a**) raw material; (**b**) 0 min; (**c**) 10 min; (**d**) 20 min and (**e**) 30 min.

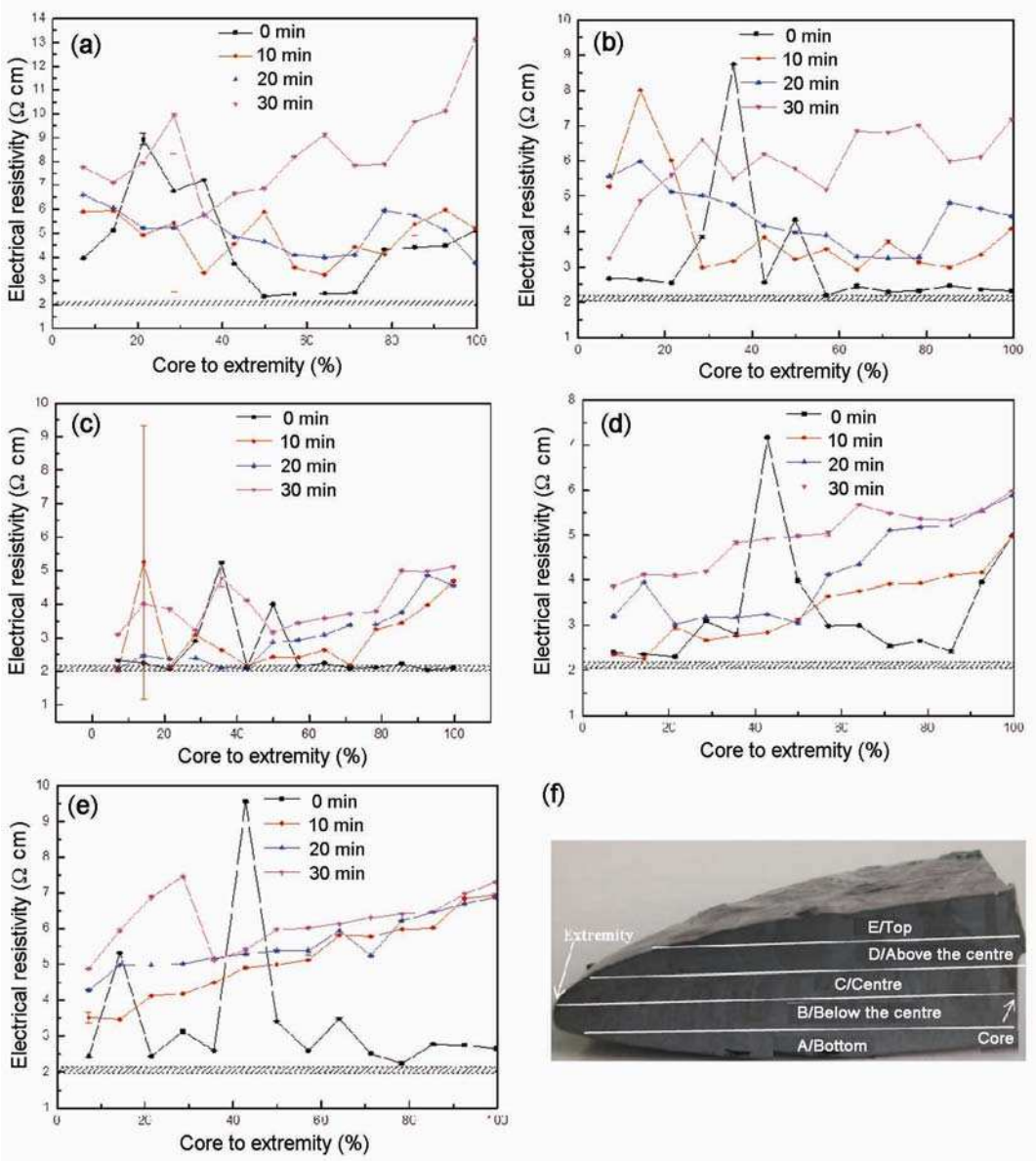

Figure 2. Average values of electrical resistivity using error bar: (**a**) at the bottom; (**b**) below the centre; (**c**) at the centre; (**d**) above the centre; (**e**) at the top and (**f**) the regions of the cross-section of the quarter sample.

regions from bottom to top through the centre. The average electrical resistivity was measured for all five regions of the samples, shown in figure 2f. Figure 2a represents the electrical resistivity graph for the bottom region along the core to the extremity of the ingot. The figure shows a visible increase in the electrical resistivity with the increase in melting time. Similarly, the peripheral areas had a notably higher value of electrical resistivity than the core area for the sample corresponding to the 30 min melting time. The average value of electrical resistivity for this sample 13.14 Ω cm was observed for 30 min melting time and this corresponded to the peripheral or extremity location. The electrical resistivity of all locations of the bottom region for all melting times is higher than the average value of raw material.

The corresponding plots (figure 2b–e) for other regions show the similar trend between electrical resistivity with melting time. That is for all regions, the electrical resistivity is seen to increase with the melting time and obviously highest for the sample with 30 min melting time. The magnitudes of electrical resistivity from the bottom to the top are 13.147, 7.18, 5.107, 5.99 and 7.3 Ω cm. Thus, the magnitude of electrical resistivity is highest for bottom region and lowest for the centre. Also, the average electrical resistivity is generally higher in extremity than in the core for all these regions.

Figure 3 illustrates the graph of electrical resistivity as a function of melting time for all the regions. For a given region, the average of electrical resistivity is calculated for the values from core to extremity and then plotted against melting time. It clearly shows that electrical resistivity increases with the melting time. Moreover, the electrical resistivity is observed to be higher at the top and bottom positions than at the centre. For higher values of melting times, the oxygen removal process is found to be more pronounced for all the regions. Hence, it also proves that oxygen is reduced more than 99.08% during 20–30 min melting time. This would be helpful in making the multicrystalline solar cells more efficient and long lasting.

3.3 *Effect of impurities on electrical resistivity distribution*

Figure 4 illustrates mechanisms of impurity transportation in silicon melt. During the melting process, the oxygen atoms are transported onto the melt surface and react with the surface silicon atoms to produce SiO gas[23]

$$\mathrm{Si\ (l) + O\ (m) = SiO\ (g)},$$

where the symbols (l), (m) and (g) denote liquid phase, concentration inside the melt and gas phase, respectively.

The saturated vapour pressure of pure substance is only a function of temperature. As for SiO, it increases from 2.79×10^2 to 4.18×10^6 Pa when the temperature changes from 1600 to 2600 K.[24] After SiO formation, the resultant SiO gas evaporates from the melted surface, which is regarded as a main mechanism for oxygen removal. During melting process, silicon is melted for a long time at a high temperature, so oxygen can be removed efficiently, leading to the increase in the average electrical resistivity.

The variation in the electrical resistivity value for the end regions and the centre region may owe to the EBM principle. A very small amount of metal impurities like Fe, Ca and Al with their low segregation coefficients

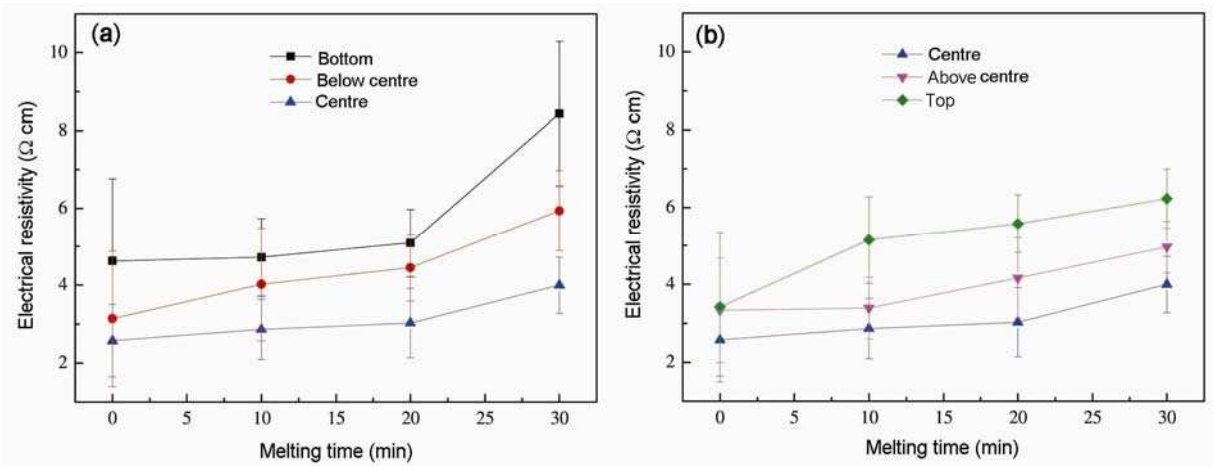

Figure 3. Depth profile of the average values of electrical resistivity is the function of time: (**a**) the lower half of the ingot and (**b**) the upper half of the ingot.

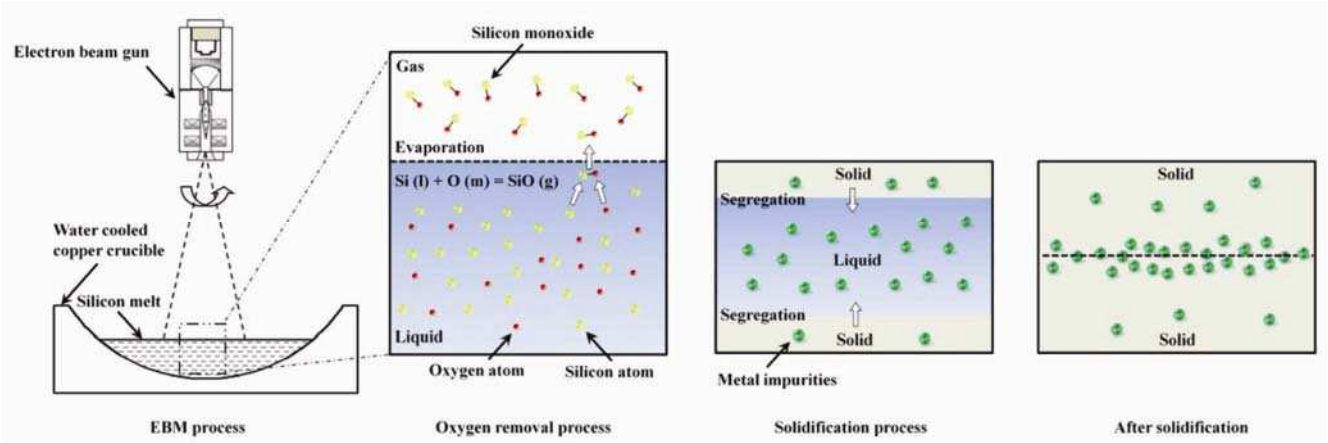

Figure 4. Mechanisms of impurity transportation in silicon melt.

0.000008, 0.008 and 0.002, respectively, still exist in the casted ingot. The distribution of above-said metal impurities are also nonuniform. During solidification in the EBM process and due to the segregation effect these metal impurities reside in the central region of the melting ingot, which is due to the EBM principle. The top and the bottom regions of the ingot solidify prior to the central region, which is because the segregation coefficients of metal impurities are very low, but on the other hand the segregation coefficient of oxygen is 1.25. Therefore, the oxygen distribution in the melting ingot is homogeneous. The value of electrical resistivity is increased altogether in the melting ingot with the increase in melting time, which is because of the removal of oxygen during EBM process. Due to very low segregation effect and EBM solidification principle, it mainly moves towards the centre and remains nonhomogeneous. However, due to the metal impurities in the central region, the value of electrical resistivity is less than that of top and the bottom.

4. Conclusions

The oxygen content was reduced from 6.177 to less than 0.0517 ppmw when refining time exceeded 10 min with removal efficiency of more than 99.08%. The electrical resistivity value of silicon was recorded 2.25 Ω cm in raw material but with the increase in melting time, the electrical resistivity of silicon was as high as between 4 and 13 Ω cm. The more interesting fact is the electrical resistivity values at the bottom of the ingot were observed to be greater than at the top. The value of electrical resistivity in the centre was less than that of top and bottom because of the presence of metal impurities, which resided because of having low segregation coefficient; while, the oxygen distribution in the ingot was homogeneous. All these verify that the increase of melting time results in an increase in oxygen removal efficiency and rise in the electrical resistivity. With all these we can increase the efficiency and the lifetime of the multicrystalline solar cell.

Acknowledgements

We gratefully acknowledge the financial support from National Key Technology R&D Program (Grant no. 2011BAE03B01), the National Natural Science Foundation of China (Grant no. U1137601) and Specialized Research Fund for the Doctoral Program of Higher Education (Grant no. 20130041110004).

References

1. Moller H J, Long L, Werner M and Yang D 1999 *Phys. Status Solidi A* **171** 175
2. Moller H J, Funke C, Lawerenz A, Riedel S and Werner M 2002 *Sol. Energy Mater. Sol. Cells* **72** 403
3. Bolotov V V, Efremov M D, Babanskaya I and Schmalz K 1993 *Mater. Sci. Eng. B – Solid* **21** 49
4. Karg D, Pensl G, Schulz M, Hassler C and Koch W 2000 *Phys. Status Solidi B* **222** 379
5. Yang D R, Li L B, Ma X Y, Fan R X, Que D L and Moeller H J 2000 *Sol. Energy Mater. Sol. Cells* **62** 37
6. Martinuzzi S and Perichaud I 1994 *Mater. Sci. Forum* **143** 1629
7. Tempelhoff K, Spiegelberg F, Gleichmann R and Wruck D 1979 *Phys. Status Solidi A* **56** 213
8. Nauka K, Gatos H C and Lagowski 1983 *J. Appl. Phys. Lett.* **43** 241
9. Bornside D E, Brown R A, Fujiwara T, Fujiwara H and Kubo T 1995 *J. Electrochem. Soc.* **142** 2790
10. Gosele U and Tan T Y 1982 *Appl. Phys. A – Mater.* **28** 79
11. Lee S T and Fellinger P 1986 *Appl. Phys. Lett.* **49** 1793
12. Borghesi A, Pivac B, Sassella A and Stella A 1995 *J. Appl. Phys.* **77** 4169
13. Jones R 2008 *Solid State Phenom.* **131–133** 225
14. Feklisova O V, Mariani-Regula G, Pichaud B and Yakimov E B 1999 *Phys. Status Solidi A* **171** 341
15. Schmidt J 2004 *Solid State Phenom.* **95–96** 187
16. Schmidt J and Bothe K 2004 *Phys. Rev. B* **69** 024107
17. Jiang D C, Shi S, Tan Y, Pang D Y and Dong W 2013 *Vacuum* **96** 27
18. Tan Y, Wen S T, Shi S, Jiang D C, Dong W and Guo X L 2013 *Vacuum* **95** 18
19. Shi S, Dong W, Peng X, Jiang D C and Tan Y 2013 *Appl. Surf. Sci.* **266** 344
20. Tan Y, Guo X L, Shi S, Dong W and Jiang D C 2013 *Vacuum* **93** 65
21. Jiang D C, Tan Y, Shi S, Dong W, Gu Z and Zou R X 2012 *Mater. Lett.* **78** 4
22. Asghar H M N U K, Tan Y, Shi S, Jiang D C, Qin S Q, Liao J, Wen S T, Dong W and Liu Y 2014 *Appl. Phys. A – Mater.* **115** 753
23. Gao B, Nakano S and Kakimoto K 2013 *Int. J. Photoenergy* Article ID 908786
24. Carlberg T, King T B and Witt A F 1982 *J. Electrochem. Soc.* **129** 189